Time-Resolved Resonance Raman Study of the Effect of pH on the Photoreactions of 3-Benzoylpyridine in Aqueous Solution

Ming-De Li, Yong Du, Chi Shun Yeung, and David Lee Phillips*

Department of Chemistry, The University of Hong Kong, Pokfulam Road, Hong Kong, P. R. China

Received: June 26, 2009; Revised Manuscript Received: September 22, 2009

A nanosecond time-resolved resonance Raman investigation of the photoreactions of 3-benzoylpyridine (3-BPy) in different pH aqueous solutions is reported. In neutral, basic, and pH = 5 aqueous solution conditions, the photoreduction reaction from the triplet 3-BPy species is observed to produce the corresponding 3-phenyl pyridyl ketyl radical that was also observed in a 2-propanol solvent. Under moderate acidic conditions (at pH = 3 for example), most of the 3-BPy triplet state species goes through two protonation steps at the nitrogen atom and the carbonyl oxygen atom after UV laser photolysis and then forms a short-lived hydration intermediate via a hydration reaction at the ortho position in the benzene ring. This new species is tentatively assigned to the *o*-^{3}[3-BPyH$^+$•H$_2$O] hydration species. In acidic aqueous solutions with a pH ≤ 1, the protonated triplet states of 3-BPy cations at the nitrogen atom are generated from photoexcitation of the protonated ground state and are subsequently further protonated at the carbonyl oxygen atom to form a 3-BPy-dication triplet state. This dication intermediate reacts with water molecules at the ortho position of the benzene ring to produce the *o*-^{3}[3-BPyH$^+$•H$_2$O] hydration species. The mechanisms of photoreduction observed for 3-BPy in different pH aqueous solutions were investigated using density functional theory calculations, and these results were used to help assign the intermediates observed in the experiments. The structures and properties of these species are briefly discussed, and an overall photoreaction mechanism is proposed based on the results from the time-resolved resonance Raman experiments and the density functional theory calculations.

Introduction

The photochemistry and photophysics of benzophenone (BP) and its derivatives have been extensively studied because of their intriguing electron transfer and hydrogen abstraction reactions in their excited states.[1−9] The lowest excited singlet (S_1) and triplet states typically have a small energy gap and are strongly coupled via a spin−orbit interaction that lead BP and many of its derivatives to have a very fast and efficient intersystem crossing to populate its triplet state that in some cases can act as a photosensitizer.[10,11] The substituents on the aromatic rings of BP derivatives can influence the relative energies of the lowest electronic excited states ($n\pi^*$ and $\pi\pi^*$) in both the singlet and triplet manifolds and therefore change the photophysical properties and photoreactivity of the lowest excited state.[6−14] Benzoylpyridines (BPy) are the heterocyclic homologues of bezophenone and there have been a number of studies of their photochemistry in different solvents.[15−19] In aqueous solutions, the ground and excited states pK values for the protonation of benzophenone are in the order pK(S_0) < pK(S_1) < pK(T_1).[20] The protonation of the triplet BP occurs simultaneously in acidic conditions and is then followed by a faster hydration reaction that produces short-lived hydration intermediates.[21] 2-Benzoylpyridine (2-BPy) has substantially different photochemical pathways from those of BP because of 2-BPy's lone pair electrons and the ortho position of the nitrogen atom that results in an efficient photocyclization reaction for the triplet state of 2-BPy.[22,23] However, 3-benzoylpyridine (3-BPy) and 4-benzoylpyridine (4-BPy) appear to have very similar photophysical properties to each other that are similar to BP in organic solvents and also in alkaline aqueous solutions.[16] In contrast, 3-BPy and 4-BPy exhibit different photochemical reactions in acidic solutions where only the protonated species of the 3-isomer could be observed. The protolytic interaction of the 3-BPy molecule in the excited state was previously examined by phosphorescence quenching. These results found an interesting pH dependent effect on the phosphorescence emission intensity and the lifetime of the triplet.[24] Favaro and co-workers employed nanosecond transient absorption and acid−base titration methods to study the excited state reactions and determined that there are two protonation steps for the excited state of 3-BPy. The first protonation step of the excited state for 3-BPy was observed to be at pK^* = 3.7 ± 0.2, and the second protonation step was observed at pK^* = 1.0 ± 0.5.[16] The excited state protonation reactions are very fast processes and thus difficult to study in real time. Therefore, there are few studies reported so far to investigate and characterize the photochemical reactions of the protonated excited-states for 3-BPy by time-resolved spectroscopic methods. Transient absorption spectroscopy has been utilized to study this compound but the unambiguous characterization of intermediates is difficult owing to overlapping of the broad featureless absorption bands of the intermediates which have lifetimes on similar time scales. Furthermore, there appears to be little if any structural and vibrational information available in the literature concerning the photochemical reactions of 3-BPy in aqueous solutions. Time-resolved resonance Raman (TR^3) is a powerful spectroscopic method that has been widely used to study many types of reactions to structurally characterize and identify transient species to learn more about their structural and electronic properties.[25]

To better characterize the photochemistry and the intermediates of 3-BPy in aqueous solutions, we have performed a time-

* To whom correspondence should be addressed. Tel.: 852-2859-2160. Fax: 852-2857-1586. E-mail: phillips@hkucc.hku.hk.

10.1021/jp905984w CCC: $40.75
Published on Web 10/13/2009

resolved resonance Raman (TR^3) spectroscopic investigation on 3-BPy in aqueous solutions of varying pH. TR^3 experiments were done for 3-BPy in H_2O/MeCN (1:1 by volume) mixed aqueous solution under neutral, alkaline (containing 0.05 M NaOH), and acidic conditions (containing either pH = 5, pH = 3, pH = 1 or 3 M $HClO_4$) in order to examine the electron-withdrawing effect of the heterocyclic nitrogen on the triplet state structure and properties as well as the transient species produced subsequent to the photoreaction in aqueous solution. To our knowledge, this is the first TR^3 characterization of these intermediates and dynamics for photoreactions of 3-BPy in different pH aqueous conditions. Density functional theory (DFT) calculations were performed using the (U)B3LPY method with a 6-311G** basis set to discern the most likely reaction pathway and to help determine the optimized structures and vibrational frequencies of the intermediate species. These results were compared with experimental data to help make assignments to the experimental vibrational bands. The structures and properties of the intermediates studied are briefly discussed and an overall photoreaction mechanism is proposed on the basis of the results from the TR^3 experiments and the DFT calculations.

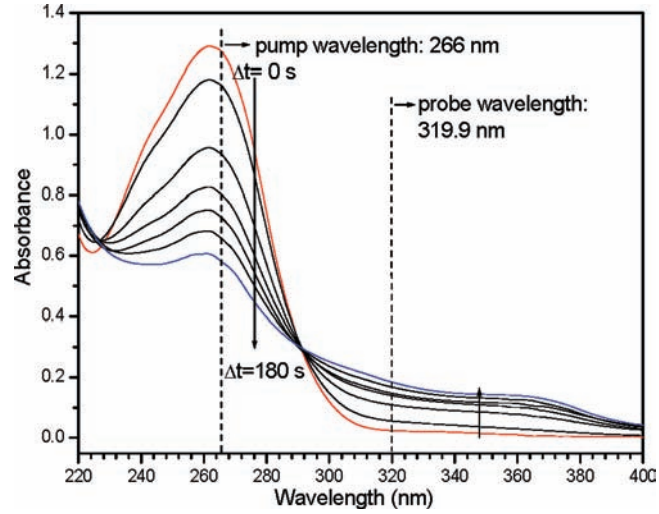

Figure 1. Absorption spectra observed after varying irradiation times using 266 nm laser photolysis of 0.05 mM 3-BPy in neutral CH_3CN:H_2O (1:1) solution. The cell path length is 10 mm. Irradiation time: 0 (red line), 30, 60, 90, 120, 150, and 180 s (blue line).

Experimental and Computational Methods

3-Benzoylpyridine was commercially obtained from Aldrich (with >99% purity) and was used as received in the experiments. Spectroscopic grade acetonitrile (MeCN) and deionized water were used as solvents for the experiments presented in this work. NaOH and $HClO_4$ were used to vary the pH value of the aqueous solutions used in all of the experiments reported here.

The nanosecond TR^3 measurements were done using an experimental apparatus and methods described previously.[25] The 266 nm pump wavelength was supplied by the fourth harmonic of a Nd:YAG laser. The 319.9 nm probe wavelength came from the second Stokes of a hydrogen Raman shifted line pumped by the second harmonic (532 nm) from a second Nd:YAG laser. The time delay between the pump and probe beam was controlled electronically by a pulse delay generator and the time resolution of the experiments was ~10 ns. The energy of the pump and the probe pulses were in the 2.5−3.5 mJ range with a repetition rate of 10 Hz. A near collinear geometry was employed to focus the pump and probe beams onto a flowing liquid stream of sample. The Raman scattering was collected in a backscattering configuration and detected by the liquid nitrogen cooled CCD detector with the Raman signal acquired by the CCD for 30 s before being read out to an interfaced PC computer. About 10 to 20 these readouts were added together to obtain a resonance Raman spectrum. The spectra were determined from subtraction of an appropriately scaled probe-before-pump spectrum from the corresponding pump−probe spectrum and the MeCN Raman bands were used to calibrate the TR^3 spectra with an estimated accuracy of ±5 cm^{-1} in absolute frequency. A Lorentzian function was utilized to integrate the Raman bands of interest in the TR^3 spectra so as to determine their integrated areas and the decay and growth dynamics of the species observed in the experiments.

The optimized geometries, vibrational modes, and the vibrational frequencies for the ground and triplet states of the different species observed in the photoreactions of interest were obtained from (U)B3LYP density functional theory (DFT) calculations employing a 6-311G** basis set. No imaginary frequency modes were observed at the stationary states of the optimized structures shown here. Transition states were located using the Berny algorithm. Frequency calculations at the same level of theory have also been performed to identify all of the stationary points as minima for transition states (one imaginary frequency). The Raman spectra were obtained using the default G03 method that used determination of Raman intensities from transition polarizabilities calculated by numerical differentiation, with assumed zero excitation frequency (e.g., the Placzek approximation). The calculated Raman frequencies from the UB3LYP/6-311G** computations were scaled by a factor of 0.975 to compare with the experimental Raman results in order to make vibrational assignments. Intrinsic reaction coordinates (IRC)[26] were calculated for the transition states to confirm that the relevant structures connect the two relevant minima. All of the calculations were done using the Gaussian 03 program suite.[27]

Results and Discussion

A. Resonance Raman Spectra of the Ground State in Aqueous Solutions of Varying pH. The UV photochemistry of 3-BPy in aqueous solution was examined by acquiring absorption spectra at varying irradiation times of 266 nm laser photolysis. Figure 1 displays the spectral changes observed for ~0.05 mM 3-BPy in neutral CH_3CN:H_2O (1:1) solution. The decrease of the intense $\pi\pi^*$ absorption band of the ketone chromophore (with a maximum at 261 nm) is accompanied by an increase of an absorption in the 300−400 nm region that has a maximum at 365 nm. The absorption spectra indicate that 3-BPy can be efficiently excited by 266 nm laser in neutral aqueous solution, and a 266 nm wavelength was chosen for the pump laser wavelength and 319.9 nm was used as a probe laser wavelength in the TR^3 experiments reported here (the pump and probe wavelengths are indicated by dashed lines above the absorption spectra in Figure 1).

The ground state is crucial for determining the reaction pathways under varying pH conditions in aqueous solutions. 3-BPy will be protonated in strong acidic solutions because of the presence of two basic centers (one on the heterocyclic nitrogen and the other on the carbonyl oxygen). In Figure 2, the DFT calculated spectra for the normal ground state (3-BPy) and the nitrogen-protonated species (3-BPyH^+) are compared with the resonance Raman spectra of the ground state. The resonance Raman spectra of the ground state obtained in pH ≥ 5 solutions agree very well with the DFT calculated spectra for the normal ground state (3-BPy), and the spectra in Figure 2 indicate that 3-BPy is not protonated at the nitrogen atom until

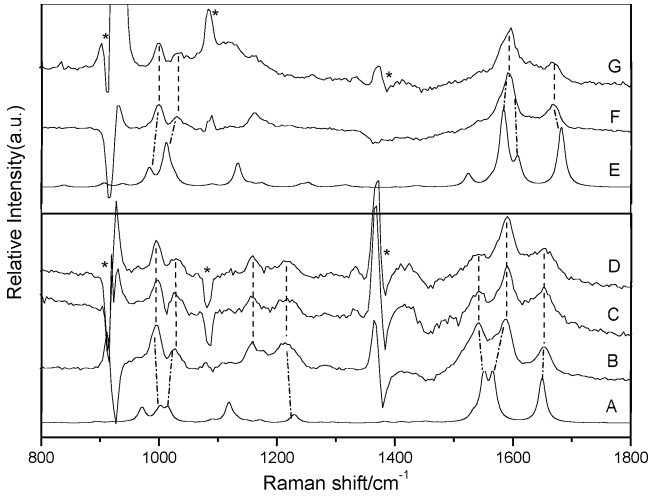

Figure 2. Compare the experimental resonance Raman spectra of 3-BPy in neutral (B), pH = 5 (C), pH = 3 (D), pH = 1 (F), and $[H^+]$ = 3 M (G) $MeCN/H_2O$ (1:1 by volume) solutions with the DFT calculated spectra for the ground state 3-BPy (A) and nitrogen-protonated 3-BPyH^+ species (E), the asterisk (*) marks subtraction artifacts. Dash lines display the correlation between the experimental and calculated Raman bands (see text for more details).

the pH value of the aqueous solution is smaller than 3. In the pH = 1 aqueous solution, the experimental Raman spectra for the ground state is consistent with the DFT calculated spectra for the nitrogen protonated species (3-BPyH^+) and this shows that 3-BPy will be protonated at the nitrogen atom and form the 3-BPyH^+ cation species at this pH. The protonation of 3-BPy likely has a significant influence on the photochemistry of 3-BPy in aqueous solutions of varying pH.

B. Time-Resolved Resonance Raman Spectroscopy of 3-BPy in Neutral, Basic, and pH = 5 Mixed Aqueous Solutions. Figure 3 displays nanosecond TR^3 spectra of 3-BPy in neutral water/acetonitrile (1:1 by volume) mixed aqueous solution acquired with various time delays that are indicated at the right side of the spectra. Inspection of Figure 3 shows that there are two intermediates observed over the 0 ns to 5 μs time scale. The first intermediate has characteristic intense Raman bands at 1541, 1216, and 994 cm^{-1}, appears promptly after photolysis, and then decays to not being observed at 100 ns. The decay of the first intermediate correlates with the growth of the intensity of the second intermediate characteristic resonance Raman bands at 1578, 1556, 1180, 1125, 1035, 1005, and 990 cm^{-1}, and this species almost completely decays within 5 μs. The first intermediate observed in the TR^3 spectra of Figure 3 is assigned to be the triplet state of 3-BPy (^{3}[3-BPy]) because it has a Raman spectrum which is essentially identical to that of the intermediate that was obtained in a neat acetonitrile solution with the same probe wavelength as used here, except that the C═C stretching vibrational mode at 1541 cm^{-1} and ring breadth stretch at 994 cm^{-1} in neutral, basic, and pH = 5 aqueous solutions shows ~6 cm^{-1} frequency upshift compared with that at 1535 and 988 cm^{-1} in neat MeCN. The comparison of these TR^3 spectra is shown in Figure 4. Since acetonitrile is an inert solvent and only the photophysical processes occur from the triplet state after laser photolysis of 3-BPy, the TR^3 spectra obtained in the neat acetonitrile enable a clear characterization of the ^{3}[3-BPy] species. To further verify the assignment of the ^{3}[3-BPy], DFT calculations were done to determine a calculated Raman spectrum, and these results are compared with the experimental resonance Raman spectra in Figure 4. Figure 4 displays a comparison between the experimental TR^3 spectra

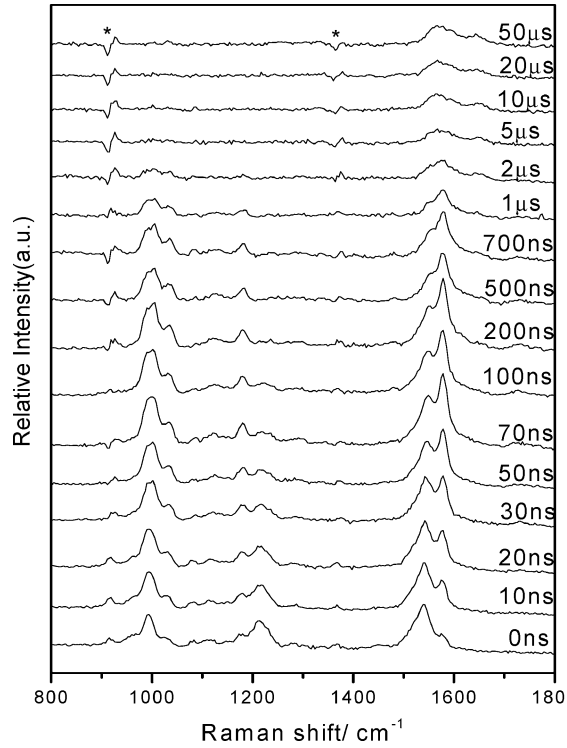

Figure 3. Nanosecond TR^3 spectra of 3-BPy in $CH_3CN:H_2O$ (1:1 by volume) obtained with a 266 nm pump excitation wavelength and a 319.9 nm probe wavelength at various delay times indicated at right side of spectra. The asterisk (*) symbols mark subtraction artifacts.

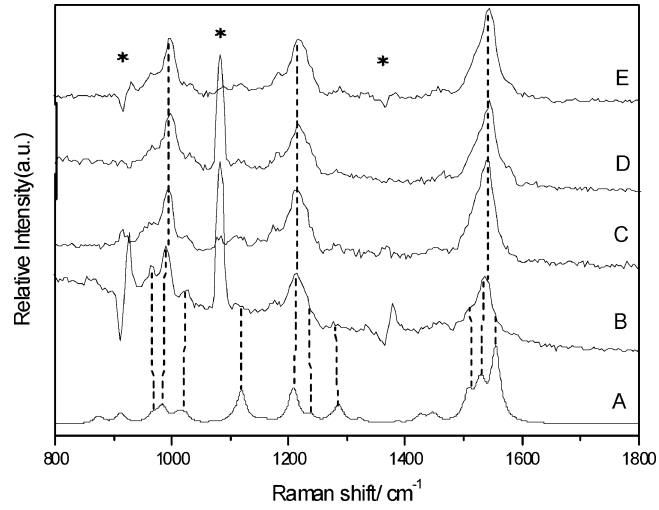

Figure 4. Comparison of the calculation predicted Raman spectra for the 3-BPy triplet state (A) with the resonance Raman spectra of the authentic 3-BPy triplet state obtained in neat acetonitrile at 5 ns (B), the first species obtained in neutral aqueous solution at 0 ns (C), the first species obtained in basic aqueous solution at 0 ns (D), and the first species obtained in pH = 5 aqueous solution at 0 ns (E). The asterisk (*) symbols mark subtraction artifacts and random laser.

obtained at 0 ns (after removing the contribution of the second species by subtracting the second species Raman spectrum using the Raman band at 1578 cm^{-1} as the marker band) in Figure 3 and the UB3LYP/6-311G** DFT-calculated normal Raman spectra of the ^{3}[3-BPy] species. This comparison reveals that the calculated Raman spectrum for the ^{3}[3-BPy] shows reasonable agreement with the experimental TR^3 spectra for the first species. The first species is therefore assigned to the ^{3}[3-BPy], and the Raman frequencies of the intense bands and their vibrational assignments are listed in Table 1S of the Supporting

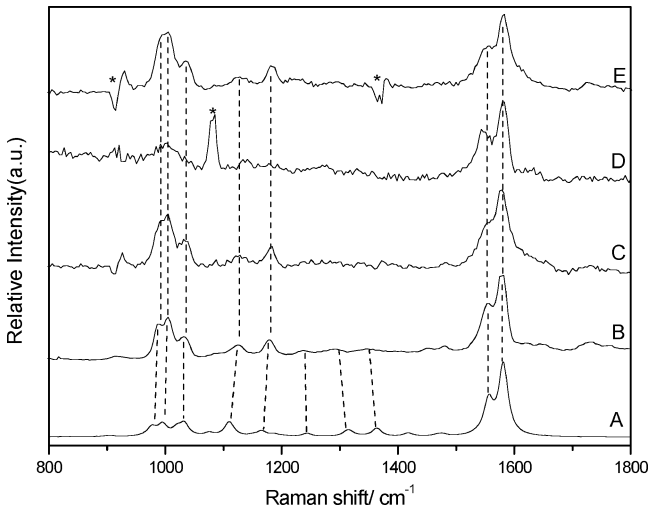

Figure 5. Comparison of the calculation predicted Raman spectrum for the ketyl radical (A) with the resonance Raman spectra of the authentic ketyl radical obtained in 2-propanol at 100 ns (B), the second species obtained in neutral aqueous solution at 500 ns (C), the second species obtained in basic aqueous solution at 500 ns (D), and the second species obtained in pH = 5 aqueous solution at 500 ns (E). The asterisk (*) symbols mark subtraction artifacts and random laser.

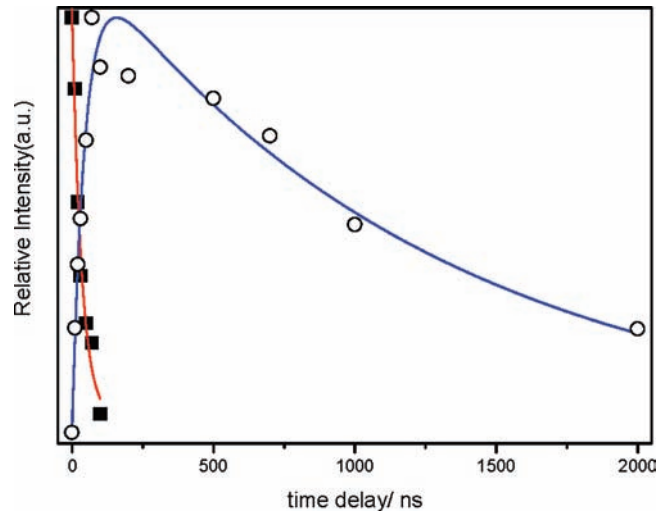

Figure 6. The time dependence of the 1216 cm^{-1} Raman band areas of the ^{3}[3-BPy] (closed squares) were fitted with a single-exponential function with a decay time constant of 33 ± 7 ns. The time dependence of the 1578 cm^{-1} Raman band areas of the second species (open circles) were fitted with a two-exponential function with a ~45 ns growth time constant and a ~1259 ns decay time constant. The data displayed here are derived from the TR^3 spectra shown in Figure 3.

Information. Figure 1S shows the optimized structure for the ^{3}[3-BPy] and this demonstrates that the substituent nitrogen atom in 3-BPy only causes some modest perturbations on the overall structure compared to that of ^{3}BP whose optimized structure is given in Figure 2S of the Supporting Information.

As mentioned above, the 3-BPy triplet state decays and forms the second species and the TR^3 spectrum at 500 ns is due to the second species. Comparison in Figure 5 of the 500 ns TR^3 spectrum of the second species with that of the intermediate obtained in the pure isopropyl alcohol with the same probe wavelength used here clearly shows that the spectra of the second species in neutral aqueous solution are essentially identical to that of the authentic 3-BPy ketyl radical obtained in the neat isopropyl alcohol solvent by the triplet state hydrogen abstraction reaction. DFT calculations have also been done to help assign the second species, and Figure 5 indicates that calculated normal Raman spectra for the 3-BPy ketyl radical shows good agreement with the experimental spectra of the second species. The second species is therefore assigned to the 3-BPy ketyl radical produced by the triplet state hydrogen abstraction reaction with water. The Raman frequencies of the main Raman bands and vibrational assignments of the 3-BPy ketyl radical are given in Table 1S and the optimized structure of the 3-BPy ketyl radical is displayed in Figure 3S in the Supporting Information. Although the ketyl radical is typically generated in hydrogen-donor solvents, such as alcohols and amines, the observation of the 3-BPy ketyl radical here in a neutral aqueous solution is consistent with similar photoreactions observed for benzophenone in neutral aqueous solution.[28]

To obtain the kinetics of first species and the second species, the contributions from other intermediates including the ^{3}[3-BPy] species or the ketyl radical species generated at post time delays need to be removed. For instance, the Raman spectra of the ^{3}[3-BPy] species were extracted by employing the characteristic 1578 cm^{-1} Raman features as a marker in Figure 3 for the 3-BPy ketyl radical and subtracting its spectrum from the TR^3 spectra obtained in the neutral solution. In the same way, the Raman spectra of the 3-BPy ketyl radical are extracted by using the characteristic 1216 cm^{-1} Raman features in Figure 3 as a marker for the ^{3}[3-BPy] species and by subtracting its spectrum from the TR^3 spectra obtained in neutral solution. The characteristic 1216 and 1578 cm^{-1} Raman features for the ^{3}[3-BPy] and 3-BPy ketyl radical species are fitted with Lorentzian band shapes to obtain the kinetics of these two species. The characteristics 1216 cm^{-1} Raman band for the ^{3}[3-BPy] was fitted with a single-exponential function with a decay time constant of ~33 ± 7 ns, the characteristic 1578 cm^{-1} Raman band of the 3-BPy ketyl radical was fitted with a two-exponential function with a ~45 ns growth time constant and a ~1259 ns decay time constant (a diagram of the kinetics is displayed in Figure 6). The time constant for the decay of the ^{3}[3-BPy] is close to the time constant for the growth of 3-BPy ketyl radical within the uncertainty of the experimental measurements and this further confirms that the ^{3}[3-BPy] is the precursor for the formation of the 3-BPy ketyl radical.

The photochemistry of 3-BPy observed in CH_3CN/H_2O mixtures shows behavior similar to that of BP. Acetonitrile is an inert solvent and 3-BPy experiences only photophysical reactions and only the triplet state of 3-BPy is observed up to a 300 ns time delay range in the neat acetonitrile solvent. However, the triplet state of 3-BPy will react with the surrounding water molecules in mixed aqueous and aqueous solutions. To examine the influence of water molecules, TR^3 experiments for 3-BPy were also done in 9:1 $MeCN/H_2O$ and 1:9 $MeCH/H_2O$ mixed solvents and there TR^3 spectra are displayed in Figure 4S of the Supporting Information. Examination of Figure 4S and Figure 3 indicates that water molecules have an obvious influence on the generation of the 3-BPy ketyl radical with the higher the concentration of water molecules leading to a larger amount of 3-BPy ketyl radical being produced. In solvents with very high concentrations of water (such as water/acetonitrile ≥9:1, v/v), the Raman intensity and lifetime of the 3-BPy radical both increase compared with that obtained at a relatively low concentration of water.

After the decay of the 3-BPy ketyl radical, a new species with a very weak Raman signal can be observed. It seems difficult to assign this species because only three Raman bands appear at 1568, 1591, and 1648 cm^{-1}. The hydrogen abstraction

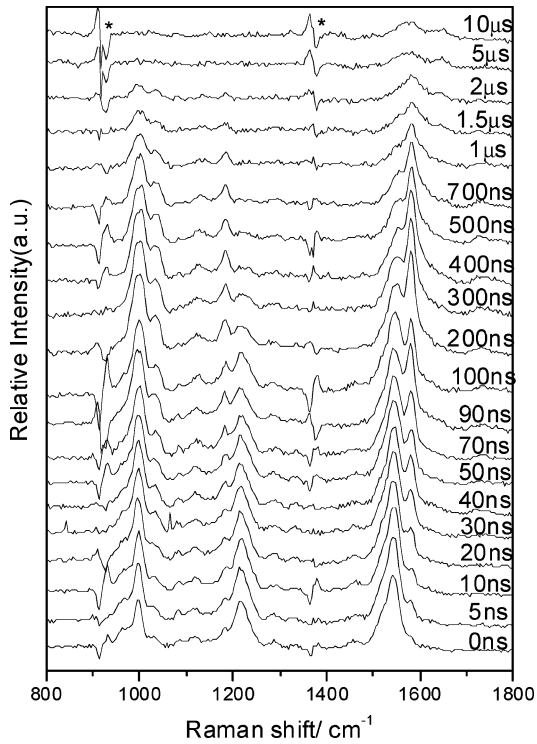

Figure 7. Nanosecond TR^3 spectra of 3-BPy in a weak acidic aqueous solution (pH = 5, CH_3CN/H_2O (1:1 by volume)) obtained with a 266 nm pump excitation wavelength and a 319.9 nm probe wavelength at various delay times that are indicated to the right of the spectra. The asterisk (*) symbols mark subtraction artifacts.

from water by the ^{3}BP produces an OH radical which then can attack BP to generate an analogous light-absorbing transients (LAT) species.[28] Because the third species can last for a very long time and 3-BPy is a BP derivative with a nitrogen atom substituent on the aromatic ring, the third species could be produced by an OH radical attacking the para position in the unsubstituted ring from a 3-BPy ketyl radical similar to the analogous reaction observed in the aqueous photochemistry of BP.[28] In neutral aqueous solution, as the 3-BPy ketyl radical decays, the third species is generated and is tentatively assigned to the 4-(hydroxyl-pyridyl-methylene)-cyclohexa-2,5-dienol species.

The TR^3 experiments for 3-BPy were also conducted in alkaline aqueous solution (which contained 0.05 M NaOH) and slight acid solution (with a pH = 5). Figure 5S of the Supporting Information and Figure 7 show that the TR^3 spectra obtained in both solutions are very similar to that obtained in neutral aqueous solution with both the ^{3}[3-BPy] and 3-BPy ketyl radical being observed. This indicates that the photochemical mechanism of 3-BPy in alkaline and slightly acidic aqueous solutions is likely the same as that of the neutral aqueous solution. This is also in good agreement with the resonance Raman spectra of the ground state obtained in these three types of solutions. Examination of Figure 5S shows that the 3-BPy ketyl radical in alkaline solution (decay time constant of ~914 ns) decays faster than that in neutral solution (decay time constant of ~1259 ns) and this suggests that the 3-BPy ketyl radical exhibits a greater reactivity toward hydroxyl ions than hydroxyl radicals. The 3-BPy ketyl radical appears more likely to couple with the surrounding hydroxyl ions and shortens the lifetime of the 3-BPy ketyl radical in alkaline aqueous solutions. Inspection of Figure 6S of the Supporting Information reveals that the ^{3}[3-BPy] has a longer lifetime (decay time constant of ~116 ns) in the pH = 5 aqueous solution than in the neutral (decay time constant of ~33 ns) and alkaline aqueous solutions (decay time constant of 40 ns) while the 3-BPy ketyl radical decays faster (decay time constant of ~922 ns) in a slightly acidic solution (pH = 5) than in the neutral aqueous solution.

C. Time-Resolved Resonance Raman Spectroscopy of 3-BPy in a pH = 3 Mixed Aqueous Solution. The ground state dissociation constant of the pyridinium cations derived from 3-BPy was previously reported to be pK_1 = ~3.0, and this makes it a possibility that pH = 3 is near a point where the photochemistry of 3-BPy will exhibit some different pathways due to the protonation of the pyridine ring in 3-BPy.[16] As shown in Figure 2, the resonance Raman spectra of the ground state indicates that 3-BPy is not protonated on the nitrogen atom in the pH = 3 mixed aqueous solution. Figure 8A displays the nanosecond TR^3 spectra of 3-BPy in a pH = 3 mixed aqueous solution acquired with various time delays that are indicated to the right of the spectra. The TR^3 spectra of 3-BPy in a pH = 3 aqueous solution are substantially different from those obtained in pH = 5 aqueous solutions. The characteristic Raman bands for the ^{3}[3-BPy] still appear at 1542, 1216, and 994 cm^{-1} and decay from around 0−200 ns. As the ^{3}[3-BPy] decays, the intensity of four resonance Raman bands (998, 1031, 1140, and 1184 cm^{-1}) gradually increase and the 1542 cm^{-1} Raman band gradually shifts down to 1531 cm^{-1} while the 1579 cm^{-1} Raman band gradually shifts up to 1594 cm^{-1}. Examination of the TR^3 spectra in Figure 8A shows that in addition to the ^{3}[3-BPy] there are still some other species observed at 0 ns time delay. An extracted Raman spectrum at 0 ns obtained by removing the contributions from the ^{3}[3-BPy] is compared with a Raman spectrum of the 3-BPy ketyl radical (see Figure 8S, Supporting Information) and it can be seen that the extracted Raman spectrum has good agreement with that of the 3-BPy ketyl radical, indicating that the 3-BPy ketyl radical is generated after the decay of the ^{3}[3-BPy]. As the delay time increases from 0 to 700 ns, the most obvious feature of the TR^3 spectra (see Figure 8A) is that the Raman band of 1579 cm^{-1} gradually shifts up to 1594 cm^{-1}, and the intensity of this band gradually increases. Figure 7S shows the differences between the resonance Raman spectra of 3-BPy obtained in the pH = 3 acidic solution at a time delay of 80 ns and the second species (ketyl radical) obtained in neutral solution at a time delay of 70 ns. This demonstrates that there are two pathways for the decay of the ^{3}[3-BPy], one pathway produces the 3-BPy ketyl radical and the other generates a new species. Figure 8B shows the extracted TR^3 spectra obtained from those acquired after photolysis of 3-BPy in a pH = 3 acidic aqueous solution (spectra shown in Figure 8A) by removing the contribution of the 3-BPy ketyl radical. The new species which has characteristic resonance Raman bands at 998, 1031, 1140, 1184, 1291, 1526, and 1594 cm^{-1} begin to appear at around 5 ns and disappear at about 3 μs. The integrated areas of the characteristic 1216 and 1594 cm^{-1} Raman bands in Figure 8B for the ^{3}[3-BPy] and the new species were determined and then fitted with a single-exponential and two-exponential functions, respectively, to obtain the time dependences of these two species. The kinetics obtained from this analysis is displayed in Figure 9. The ^{3}[3-BPy] has a decay time constant of 48 ± 10 ns and the new species has a growth time constant of ~138 ns and a decay time constant of ~1518 ns. The time constant for the decay of the ^{3}[3-BPy] (48 ± 10 ns) is far shorter than the time constant for the growth of the new species and this suggests there are two pathways for the decay of the ^{3}[3-BPy] as mentioned before. The time constant for the growth of the 3-BPy ketyl radical can be approximately

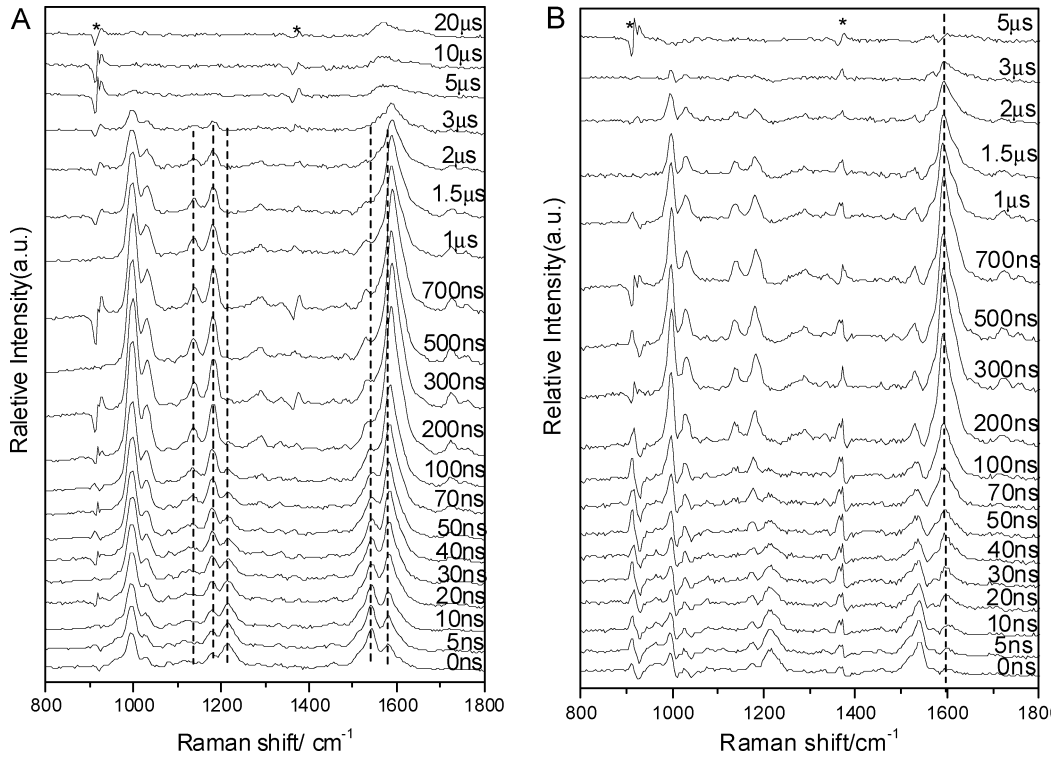

Figure 8. (A) Nanosecond TR[3] spectra of 3-BPy in a pH = 3 acidic aqueous solution (CH_3CN/H_2O (1:1 by volume)) obtained with a 266 nm pump excitation wavelength and a 319.9 nm probe wavelength at various delay times that are indicated to the right of the spectra and (B) the extracted TR[3] spectra obtained from those spectra acquired after photolysis of 3-BPy in a pH = 3 acidic aqueous solution (spectra shown in panel A) by removing the contribution of the ketyl radical species. The asterisk (*) symbols mark subtraction artifacts.

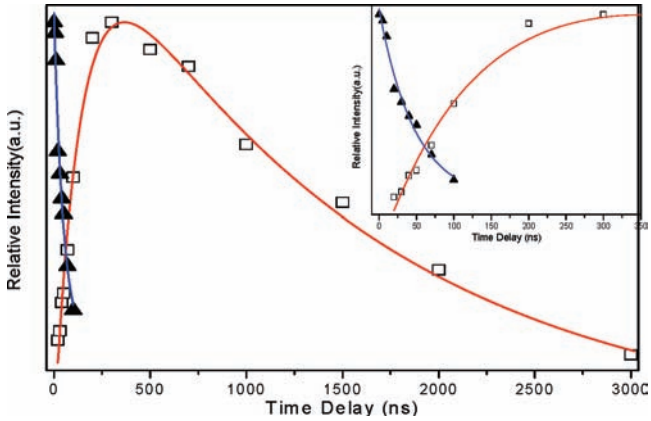

Figure 9. The time dependence of the 1216 cm^{-1} Raman band integrated areas of the ^{3}[3-BPy] (closed triangles) were fitted with a single-exponential function with a decay time constant of 48 ± 10 ns. The time dependence of the 1594 cm^{-1} Raman band areas of the new species (opened squares) were fitted with a two-exponential function with a ~138 ns growth time constant and a ~1518 ns decay time constant. The inset displays an expanded view of the kinetics during the first 300 ns. The data displayed here were derived from the TR[3] spectra shown in Figure 8B.

estimated by the rate equation of reaction 1. So the time constant for the growth of the 3-BPy ketyl radical is approximately 74 ns.

$$k_{\text{decay of 3-BPy triplet state}} = k_{\text{growth of ketyl radical}} + k_{\text{growth of new species}} \quad (1)$$

Because of the relatively long lifetime of the triplet state, which generally allows an acid−base equilibrium in the exited state to be attained, a triplet−triplet absorption titration indicated that the dissociation constant for the first protonation step of the ^{3}[3-BPy] on the nitrogen atom of the pyridinium cations is $pK_1^* = 3.7$.[16] Thus, irradiation of 3-BPy in a pH = 3 aqueous solution, a small part of the ^{3}[3-BPy] couples with water to form the 3-BPy ketyl radical through the hydrogen abstraction reaction, but the majority of the ^{3}[3-BPy] is protonated at the nitrogen atom to form the triplet state of the 3-BPy cation (^{3}[3-BPyH$^+$]), which is a shorter-lived species than the basic ones in the excited state. The ^{3}[3-BPyH$^+$] species is likely to be further protonated on the carbonyl oxygen to form the triplet state of the 3-BPy-dication just like the protonation of BP in acid solution.[28] As the triplet state of the 3-BPy-dications decay a new species is generated.

D. Time-Resolved Resonance Raman Spectroscopy of 3-BPy in a pH ≤ 1 Mixed Aqueous Solutions: Observation of the Photohydration Products after Photolysis of 3-BPy in Strong Acidic Aqueous Solution. The ground state resonance Raman spectra of 3-BPy demonstrates that 3-BPy is protonated at the nitrogen atom and forms the 3-BPyH$^+$ cation in pH = 1 and [H$^+$] = 3 M aqueous solutions. This is consistent with the ground state dissociation constant of the pyridinium cations ($pK_1 = \sim 3$). Since the protonation of the carbonyl group is negligible in these two aqueous solutions due to $pK_2 < -6$,[16] the majority of the molecules excited in these solutions should be the ground state of the 3-BPyH$^+$ cation. Figure 9S shows the TR[3] spectra obtained in a pH = 1 aqueous solution at various time delay. The ^{3}[3-BPy] is not observed within the resolution of the TR[3] apparatus used here and this suggests that the 3-BPyH$^+$ cations account for most of the ground state species and are excited to the triplet state of the 3-BPyH$^+$ cations (^{3}[3-BPyH$^+$]), which is a shorter lived intermediate than the ^{3}[3-BPy] species. Thus, the Raman signals of the ^{3}[3-BPyH$^+$] may not be observed since the lifetime of ^{3}[3-BPy•H$^+$] is shorter than the time resolution of the nanosecond TR[3] experimental

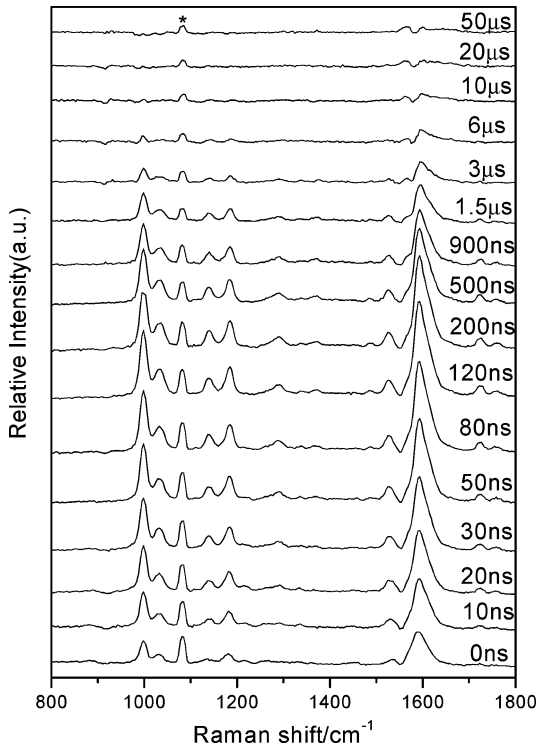

Figure 10. The extracted TR^3 spectra obtained from those spectra acquired after photolysis of 3-BPy in a pH = 1 acidic aqueous solution (spectra shown in Figure 9S, Supporting Information.) by removing the contribution of the ketyl radical species. All of the spectra were obtained with a 266 nm pump excitation wavelength and a 319.9 nm probe wavelength. The asterisk (*) symbols mark subtraction artifacts and random laser.

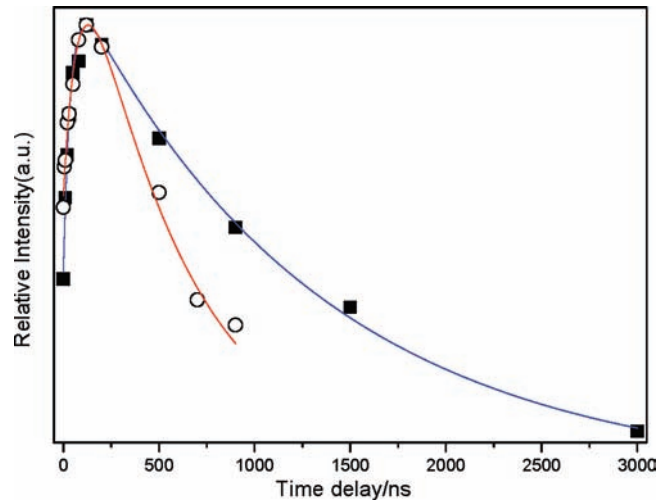

Figure 11. The time dependence of the 1596 cm^{-1} Raman band areas of o-^{3}[3-$BPyH^+ \cdot H_2O$] (closed squares) under open air conditions were fitted with a two-exponential function with a ~39 ns growth time constant and a ~1290 ns decay time constant. The time dependence of the 1596 cm^{-1} Raman band areas of o-^{3}[3-$BPyH^+ \cdot H_2O$] (open circles) under O_2 purging conditions were fitted with a two-exponential function with a ~79 ns growth time constant and a ~535 ns decay time constant. The data displayed here are derived from the TR^3 spectra shown in Figure 10 and Figure 10S.

apparatus employed here. Although most of the 3-BPy compound is protonated to form the 3-$BPyH^+$ cation in the pH = 1 aqueous solution, we cannot completely ignore the presence of a modest amount of the unprotonated 3-BPy species. A small part of the 3-BPy compound will be excited to the ^{3}[3-BPy] intermediate and then undergo a hydrogen abstraction to form some 3-BPy ketyl radical species.

To obtain the TR^3 spectra of the new species, the contribution of the 3-BPy ketyl radical needs to be removed. The extracted TR^3 spectra show that only one new species is observed from 0 ns to 3 μs which has characteristic resonance Raman bands at 998, 1031, 1140, 1184, 1291, 1531, and 1594 cm^{-1}. Consequently, this new species and the species that was also obtained at a time delay of 700 ns in the pH = 3 aqueous solution are the same one. The 1594 cm^{-1} Raman feature for the new species in Figure 10 was fitted with Lorentzian band shapes to obtain the time dependences of the integrated Raman band areas of the new species and Figure 11 displays the kinetics of associated with this new species. This species has a very short growth time constant of ~39 ns and a long decay time constant of ~1290 ns and this indicates that the ^{3}[3-$BPyH^+$] intermediates are easy to undergo further protonation in a pH = 1 aqueous solution to form the 3-BPy-dication triplet state species. The 3-BPy-dication triplet state intermediate is very unstable and appears to react with water molecules to produce a triplet hydration product. This is consistent with BP that the protonated BP triplet state (^{3}[$BP \cdot H^+$]) can be easily attacked by water molecule to form two triplet hydration products (m-$^3BP \cdot H_2O$ and o-$^3BP \cdot H_2O$) in acid aqueous solution.[28] To verify this new species is a triplet state or a single state, experiments with oxygen purging were performed (these TR^3 spectra are displayed in Figure 10S, Supporting Information) and plots of the integrated areas for the strongest Raman band at 1594 cm^{-1} as the function of time delays from 0 ns to 1.2 μs were obtained (these dynamics are displayed in Figure 11). This species was found to be sensitive to oxygen and has its lifetime shortened from ~1290 to ~535 ns. Therefore this intermediate is thought to have triplet character.

Water molecules may attack different positions of the benzene ring or the pyridine ring in 3-BPy-dication triplet state and Scheme 1S, Supporting Information shows nine possible triplet hydration reaction pathways of the 3-BPy-dication triplet state. To help to assign this new species, DFT calculations (UB3LPY/6-311**) were carried out to predict the Raman spectra for those nine triplet hydration products. The results indicate that the RX-o reaction pathway is the most feasible one and water molecules prefer to attack the ortho position of the benzene ring for the 3-BPy-dication triplet state (the RX-o reaction pathway is displayed in Scheme 1S) to form the o-^{3}[3-$BPyH^+ \cdot H_2O$] hydration product. Comparison of the resonance Raman spectrum of the new species obtained in the pH = 3 acidic aqueous solution at 700 ns with the TR^3 spectrum of the new species obtained in a pH = 1 acidic aqueous solution at 80 ns and also with the DFT predicted Raman spectrum for the o-^{3}[3-$BPyH^+ \cdot H_2O$] species are displayed in Figure 12. The DFT calculation predicted Raman spectra of the o-^{3}[3-$BPyH^+ \cdot H_2O$] species shows reasonable agreement with the TR^3 spectra for the new species observed in the strong acidic aqueous solutions. The differences in the relative intensities between the calculated and experimental Raman spectra can be attributed to the fact that the spectrum predicted from the calculations is the normal Raman spectrum while the experimental spectra are resonantly enhanced spectra. The somewhat similar intensity pattern between the experimental resonance Raman spectrum and the calculated normal Raman spectrum is fortuitous. The optimized structure with selected bond lengths and bond angles indicated for o-^{3}[3-$BPyH^+ \cdot H_2O$] is illustrated in Figure 13. The major resonance Raman

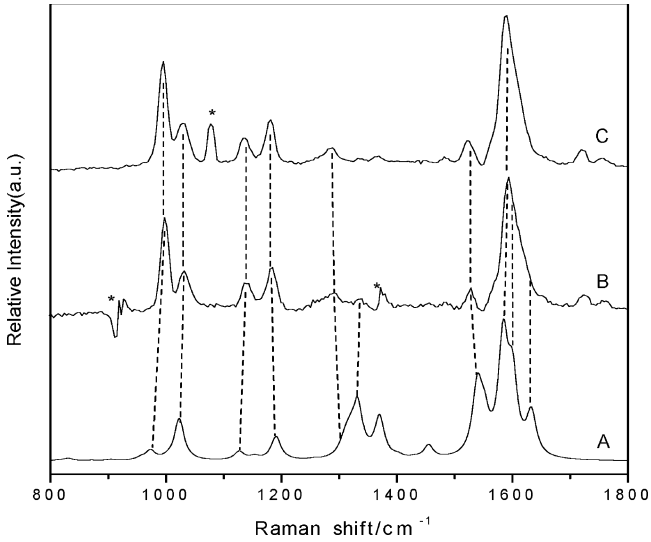

Figure 12. Comparison of resonance Raman spectra of (B) the new species obtained in a pH = 3 acidic aqueous solution at 700 ns and (C) the new species obtained in a pH = 1 acidic aqueous solution at 80 ns with (A) the DFT predicted Raman spectra for the *o*-^{3}[3-BPyH$^+$·H$_2$O] species. The asterisk (*) symbols mark subtraction artifacts and random laser.

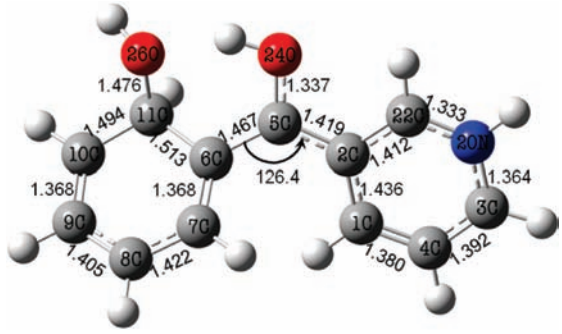

Figure 13. Optimized structure of the *o*-^{3}[3-BPyH$^+$·H$_2$O] species computed from the UB3LPY/6-311G** DFT calculations. Selected carbon positions, bond lengths (in Å), and bond angles (in degrees) are labeled.

band positions and their vibrational descriptions and tentative assignments for the *o*-^{3}[3-BPyH$^+$·H$_2$O] species is presented in Table 1S.

We also systematically compared the barriers of the nine triplet hydration reaction pathways for 3-BPy in order to find the most favorable pathway predicted from the DFT calculations. Intrinsic reaction coordinate (IRC) computations were done to confirm that the transition states connected the corresponding reactants and products. Figure 14 shows a schematic diagram of the gas-phase calculated relative free-energy barriers for the hydration reactions examined here. Inspection of Figure 14 shows that the RX-*o* pathway (water molecules attacking the ortho position of benzene ring) has a noticeably lower free-energy barrier than the other reaction pathways and is exothermic in nature. This indicates that the RX-*o* reaction pathway is both kinetically and thermodynamically the most favorable one. That this is the most feasible reaction pathway (RX-*o*) is consistent with the mechanism proposed previously for a similar reaction of BP in acidic aqueous solutions.[28] Figure 15 illustrates the schematic diagram of the optimized geometry of the reactant (RCo), the transition state (TSo), and the product (PRo) for the RX-*o* hydration reaction pathway. To explain the energy

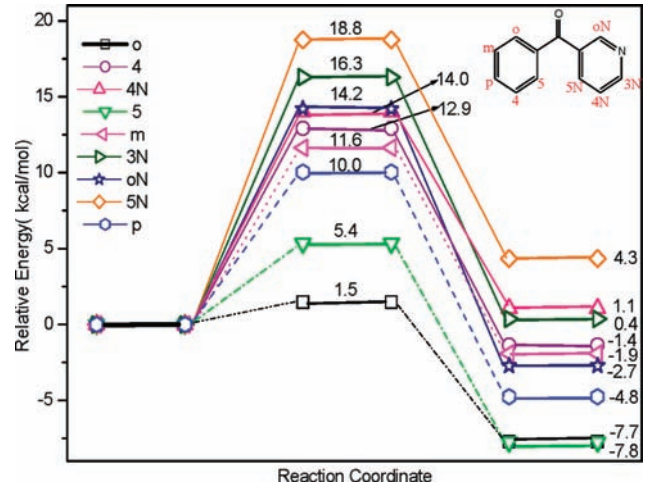

Figure 14. The relative free energy diagram for the nine hydration reaction pathways (Scheme 1S) is presented here. The top right side of the graph shows the structure of 3-benzoylpyridine with the symbols related to the nine hydration reaction pathways given next to the appropriate positions in the molecule.

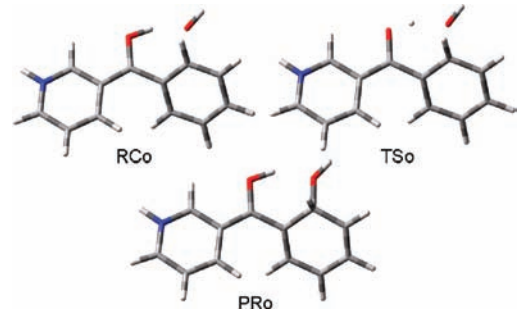

Figure 15. Schematic diagrams of the optimized geometry of RCo, TSo, and PRo.

barrier differences observed for these hydration reactions, the transition states of the different pathways were examined and we found that the transition state (TSo) involved in the RXo hydration reaction pathway has a strong hydrogen bond (1.537 Å) between the hydroxyl and the proton (attached on the carboxyl group), and this appears to drive most of the positive charge to the ortho position of the benzene ring. Therefore the ortho position is the most favorable position to be attacked by the water molecules. Inspection of the optimized geometry for PRo shows an analogous six-atom ring existing through hydrogen bonding among the $C_5-C_6-C_{11}-O_{26}-H-O_{24}$ moiety and this significantly increases the stability for the *o*-^{3}[3-BPyH$^+$·H$_2$O] species. Thus, only a small free energy barrier is required to be overcome in the RX-*o* hydration reaction pathway. Because the experiments for the hydration reaction of 3-BPy were performed in an aqueous solution, we also performed calculations that considered solvent effects on these reactions. The solvent effects on these reactions were investigated by employing the SCRF method based on a polarizable continuum model (PCM) applied on the UB3LPY/6-311G** optimized gas-phase stationary points.[29] H_2O is used as the solvent and the hydration barriers in all of the nine reaction pathways decrease with the RX-*o* pathway still having the lowest barrier among all of the hydration pathways examined. Therefore, the calculation results in both the gas and aqueous solution phases imply that the RX-*o* hydration reaction pathway is the most favorable one and this is consistent with the good agreement between the DFT predicted Raman

SCHEME 1: Proposed Mechanism for the Photochemistry of 3-BPy in Different pH Aqueous Solutions

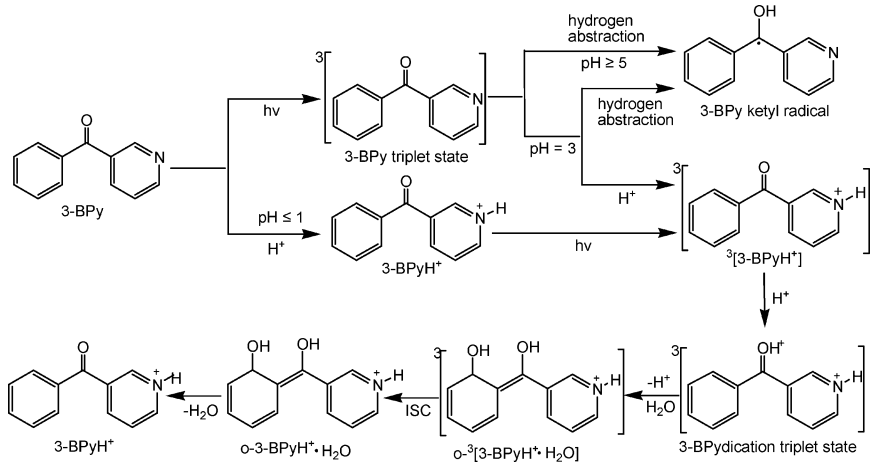

spectrum and the experimental resonance Raman spectra for the new species as shown in Figure 12.

TR^3 experiments were also carried out in a stronger acidic aqueous solution ($[H^+] = 3$ M $HClO_4$) and these TR^3 spectra are displayed in Figure 11S in the Supporting Information. The *o*-^{3}[3-$BPyH^+ \cdot H_2O$] species is also observed in the 3 M $HClO_4$ aqueous solution from 0 ns to 2 μs and the dynamics of this species was found to be the essentially the same as that obtained in the pH = 1 aqueous solution. Oxygen-purge experiments were performed and these results also demonstrated that *o*-^{3}[3-$BPyH^+ \cdot H_2O$] could be quenched by oxygen similar to results obtained in the pH = 1 experiments purged by oxygen. This further indicates that the observed species likely has triplet character.

Conclusion

Nanosecond time-resolved resonance Raman spectroscopy was used to investigate the photoreactions of 3-BPy in different pH aqueous solutions. The hydrogen abstraction reaction occurs efficiently for the 3-BPy triplet state with solvent molecules to form a 3-BPy ketyl radical species with different reaction rates after 266 nm photolysis of 3-BPy in basic, neutral, and pH = 5 aqueous solutions. However, in addition to the formation of the 3-BPy ketyl radical, the protonation of the triplet 3-BPy on the nitrogen and the oxygen atoms occur subsequently in pH = 3 aqueous solution that is then followed by a faster hydration reaction to produce the corresponding photohydration short-lived intermediate (*o*-^{3}[3-$BPyH^+ \cdot$H2O]). In pH ≤ 1 aqueous solutions, the ^{3}[3-$BPyH^+$] triplet state is generated after irrradation of its ground state and then quickly produces the 3-BPy-dication triplet state that then reacts with water molecules at the ortho position in the benzene ring to produce the *o*-^{3}[3-$BPyH^+ \cdot$H2O] hydration intermediate. DFT computational results were used to help further confirm this assignment. The DFT calculations showed that the RX-*o* hydration reaction pathway has the lowest barrier to reaction compared to the other possible pathways examined. A reaction scheme (see Scheme 1) based on the experimental and computational results reported here for the photoreaction pathways of 3-BPy in various aqueous solutions was proposed.

Acknowledgment. This research has been supported by grants from the Research Grants Council of Hong Kong (HKU 7035/08P), the award of a Croucher Foundation Senior Research Fellowship (2006−07) from the Croucher Foundation and an Outstanding Researcher Award (2006) from the University of Hong Kong to D.L.P.

Supporting Information Available: Additional Figures 1S−14S, tables, and schemes. This material is available free of charge via the Internet at http://pubs.acs.org.

References and Notes

(1) Nelson, D. A.; Hayon, E. *J. Phys. Chem.* **1972**, *76*, 3200–3207.
(2) Bensasson, R. V.; Gramain, J. C. *J. Chem. Soc., Faraday Trans. 1* **1980**, *76*, 1801–1810.
(3) Bhasikuttan, A. C.; Singh, A. K.; Palit, D. K.; Sapre, A. V.; Mittal, J. P. *J. Phys. Chem. A* **1998**, *102*, 3470–3480.
(4) Shizuka, H.; Yamaji, M. *Bull. Chem. Soc. Jpn.* **2000**, *73*, 267–280.
(5) Wagner, P. J.; Truman, R. J.; Scaiano, J. C. *J. Am. Chem. Soc.* **1985**, *107*, 7093–7097.
(6) Favaro, G. *J. Chem. Soc., Perkin Trans. 2* **1976**, 869–876.
(7) Ramseier, M.; Senn, P.; Wirz, J. *J. Phys. Chem. A* **2003**, *107*, 3305–3315.
(8) Mitchell, D.; Lukeman, M.; Lehnherr, D.; Wan, P. *Org. Lett.* **2005**, *7*, 3387–3389.
(9) Du, Y.; Ma, C. S.; Kwok, W. M.; Xue, J. D.; Phillips, D. L. *J. Org. Chem.* **2007**, *72*, 7148–7156.
(10) Shah, B. K.; Rodgers, M. A.; Neckers, D. C. *J. Phys. Chem. A* **2004**, *108*, 6087–6089.
(11) Shah, B. K.; Neckers, D. C. *J. Am. Chem. Soc.* **2004**, *126*, 1830–1835.
(12) Blanchi, J. P.; Watkins, A. R. *Mol. Photochem.* **1974**, *6*, 133–142.
(13) Bortolus, P.; Elisei, F.; Favaro, G.; Monti, S.; Ortica, F. *J. Chem. Soc., Faraday Trans.* **1996**, *92*, 1841–1851.
(14) Ortica, F.; Elisei, F.; Favaro, G. *J. Phys. Org. Chem.* **1999**, *12*, 31–38.
(15) Du, Y.; Xue, J. D.; Ma, C. S.; Kwok, W. M.; Phillips, D. L. *J. Raman Spectrosc.* **2008**, *39*, 503–514.
(16) Elisei, F.; Favaro, G.; Ortica, F. *J. Chem. Soc., Faraday Trans.* **1994**, *90*, 279–285.
(17) Albini, A.; Bortolus, P.; Fasani, E.; Monti, S.; Negri, F.; Orlandi, G. *J. Chem. Soc., Perkin Trans. 2* **1993**, 691–695.
(18) Favaro, G.; Masetti, F. *J. Phys. Chem.* **1978**, *82*, 1213–1218.
(19) Gorner, H. *Chem. Phys.* **2008**, *344*, 264–272.
(20) Rayner, D. M.; Wyatt, P. A. H. *J. Chem. Soc., Faraday Trans. 2* **1974**, *8*, 945–954.
(21) Ramseier, M.; Senn, P.; Wirz, J. *J. Phys. Chem. A* **2003**, *107*, 3305–3315.
(22) Hurt, C. R.; Filipesc, N. *J. Am. Chem. Soc.* **1972**, *94*, 3649–3651.
(23) Guan, X. G.; Du, Y.; Xue, J. D.; Phillips, D. L. *J. Phys. Chem. A* **2009**, *113*, 1999–2003.
(24) Favaro, G.; Masetti, F.; Romani, A. *Spectrosc. Acta A* **1989**, *45*, 339–346.
(25) (a) Zhu, P.; Ong, S. Y.; Chan, P. Y.; Leung, K. H.; Phillips, D. L. *J. Am. Chem. Soc.* **2001**, *123*, 2645–2649. (b) Zhu, P.; Ong, S. Y.; Chan, P. Y.; Poon, Y. F.; Leung, K. H.; Phillips, D. L. *Chem.—Eur. J.* **2001**, *7*, 4928–4936. (c) Li, Y.-L.; Leung, K. H.; Phillips, D. L. *J. Phys. Chem. A* **2001**, *105*, 10621–10625. (d) Chan, P. Y.; Kwok, W. M.; Lam, S. K.; Chiu, P.; Phillips, D. L. *J. Am. Chem. Soc.* **2005**, *127*, 8246–8247. (e) Xue, J.;

Chan, P. Y.; Du, Y.; Guo, Z.; Chung, C. W. Y.; Toy, P. H.; Phillips, D. L. *J. Phys. Chem. B* **2007**, *111*, 12676–12684.

(26) Fukui, K. *J. Phys. Chem.* **1970**, *74*, 4161–4163.

(27) (a) Frisch, M. J.; Trucks, G. W.; Schlegel, H. B.; Scuseria, G. E.; Robb, M. A.; Cheeseman, J. R.; Zakrzewski, V. G.; Montgomery, J. A., Jr.; Stratmann, R. E.; Burant, J. C.; Dapprich, S.; Millam, J. M.; Daniels, A. D.; Kudin, K. N.; Strain, M. C.; Farkas, O.; Tomasi, J.; Barone, V.; Cossi, M.; Cammi, R.; Mennucci, B.; Pomelli, C.; Adamo, C.; Clifford, S.; Ochterski, J.; Petersson, G. A.; Ayala, P. Y.; Cui, Q.; Morokuma, K.; Malick, D. K.; Rabuck, A. D.; Raghavachari, K.; Foresman, J. B.; Cioslowski, J.; Ortiz, J. V.; Stefanov, B. B.; Liu, G.; Liashenko, A.; Piskorz, P.; Komaromi, I.; Gomperts, R.; Martin, R. L.; Fox, D. J.; Keith, T.; Al-Laham, M. A.; Peng, C. Y.; Nanayakkara, A.; Gonzalez, C.; Challacombe, M.; Gill, P. M. W.; Johnson, B. G.; Chen, W.; Wong, M. W.; Andres, J. L.; Head-Gordon, M.; Replogle, E. S.; Pople, J. A. *Gaussian 98*, revision A.7; Gaussian Inc: Pittsburgh, PA, 1998. (b) Frisch, M. J.; Trucks, G. W.; Schlegel, H. B.; Scuseria, G. E.; Robb, M. A.; Cheeseman, J. R.; Montgomery, J. A., Jr.; Vreven, T.; Kudin, K. N.; Burant, J. C.; Millam, J. M.; Iyengar, S. S.; Tomasi, J.; Barone, V.; Mennucci, B.; Cossi, M.; Scalmani, G.; Rega, N.; Petersson, G. A.; Nakatsuji, H.; Hada, M.; Ehara, M.; Toyota, K.; Fukuda, R.; Hasegawa, J.; Ishida, M.; Nakajima, T.; Honda, Y.; Kitao, O.; Nakai, H.; Klene, M.; Li, X.; Knox, J. E.; Hratchian, H. P.; Cross, J. B.; Adamo, C.; Jaramillo, J.; Gomperts, R.; Stratmann, R. E.; Yazyev, O.; Austin, A. J.; Cammi, R.; Pomelli, C.; Ochterski, J. W.; Ayala, P. Y.; Morokuma, K.; Voth, G. A.; Salvador, P.; Dannenberg, J. J.; Zakrzewski, V. G.; Dapprich, S.; Daniels, A. D.; Strain, M. C.; Farkas, O.; Malick, D. K.; Rabuck, A. D.; Raghavachari, K.; Foresman, J. B.; Ortiz, J. V.; Cui, Q.; Baboul, A. G.; Clifford, S.; Cioslowski, J.; Stefanov, B. B.; Liu, G.; Liashenko, A.; Piskorz, P.; Komaromi, I.; Martin, R. L.; Fox, D. J.; Keith, T.; Al-Laham, M. A.; Peng, C. Y.; Nanayakkara, A.; Challacombe, M.; Gill, P. M. W.; Johnson, B.; Chen, W.; Wong, M. W.; Gonzalez, C.; Pople, J. A. *Gaussian 03*, revision B.05; Gaussian, Inc.: Wallingford, CT, 2004.

(28) Du, Y.; Xue, J. D.; Li, M. D.; Phillips, D. L. *J. Phys. Chem. A* **2009**, *113*, 3344–3352.

(29) Cances, E.; Mennucci, B.; Tomasi, J. *J. Chem. Phys.* **1997**, *107*, 3032–3041.

JP905984W